



Article

Anti-Inflammatory and Anti-Airway Remodeling Activities of Jakyakgamcho-Tang in a Mouse Model of COPD

Jee Hyun Kang ¹, Yu-Jin Kim ², Eun Bok Baek ¹, Eun-Ju Hong ¹, Mee-Young Lee ² and Hyo-Jung Kwun ^{1,*}

¹ Department of Veterinary Pathology, College of Veterinary Medicine, Chungnam National University, Daejeon 34134, Korea

² Herbal Medicine Research Division, Korea Institute of Oriental Medicine, Daejeon 34054, Korea

* Correspondence: hyojung@cnu.ac.kr; Tel.: +82-42-821-6751; Fax: +82-42-821-8903

Abstract: Jakyakgamcho-tang (JGT) is used in oriental medicine to treat inflammation and allergy. Chronic obstructive pulmonary disease (COPD) causes respiratory inflammation, airway remodeling, and pulmonary emphysema. We examine the influence of JGT on COPD by using a mouse model. COPD was induced by inhalation of cigarette smoke (CS) and nasal administration of lipopolysaccharide (LPS). In comparison to COPD mice induced by CS and LPS, mice administered with JGT exhibited significantly lower amounts of inflammatory cells and reduced expression levels of tumor necrosis factor- α (TNF- α), interleukin-6 (IL-6), IL-1 β , and monocyte chemoattractant protein-1 (MCP-1) in bronchoalveolar lavage fluid (BALF) and lung tissue. The elevated concentrations of transforming growth factor- β (TGF- β), α -smooth muscle actin (α -SMA), and matrix metalloproteinase-9 (MMP-9) induced by CS and LPS were also inhibited by JGT treatment. Moreover, JGT suppressed CS and LPS-induced phosphorylation of nuclear factor kappa B (NF- κ B), extracellular signal-regulated kinase1/2 (ERK1/2) and mitogen-activated protein kinases (p38 MAPKs). In a COPD mouse model, our results demonstrated that JGT prevented CS and LPS induced airway inflammation and remodeling.



Citation: Kang, J.H.; Kim, Y.-J.; Baek, E.B.; Hong, E.-J.; Lee, M.-Y.; Kwun, H.-J. Anti-Inflammatory and Anti-Airway Remodeling Activities of Jakyakgamcho-Tang in a Mouse Model of COPD. *Appl. Sci.* **2022**, *12*, 8646. <https://doi.org/10.3390/app12178646>

Academic Editors: Blanca Cárdbana and Jose Antonio Cañas

Received: 4 August 2022

Accepted: 25 August 2022

Published: 29 August 2022

Publisher's Note: MDPI stays neutral with regard to jurisdictional claims in published maps and institutional affiliations.



Copyright: © 2022 by the authors. Licensee MDPI, Basel, Switzerland. This article is an open access article distributed under the terms and conditions of the Creative Commons Attribution (CC BY) license (<https://creativecommons.org/licenses/by/4.0/>).

Keywords: chronic obstructive pulmonary disease; cigarette smoke; Jakyakgamcho-tang; lipopolysaccharide

1. Introduction

In chronic obstructive pulmonary disease (COPD), airflow to the lung is significantly restricted, making breathing difficult [1]. The main features of COPD are chronic bronchitis, excessive secretion of mucus, bronchiolar and vascular remodeling, pulmonary hypertension, emphysema, and pulmonary fibrosis [2]. Previous research indicated that COPD is becoming a greater public health burden worldwide because of the aging population and the increasing exposure to risk factors. During COPD, the indicators of chronic inflammation are the infiltration and fibrosis of cells, obstruction of peripheral airways, and inflammatory exudates accumulation in the lumen. The pathogenesis of COPD involves numerous proinflammatory cytokines and chemokines.

Smoking is a significant cause of COPD. Cigarette smoke (CS) contains free radicals as well as reactive chemical compounds, such as aldehydes and semiquinones [3]. During lung inflammation, neutrophils and monocytes accumulate after exposure to CS. The CS thus increases chemotaxis, cell adhesion, and phagocytosis, and the release of superoxide anions and enzyme granules [4]. COPD presently has no cure, however therapies such as quitting smoking, using inhalers and pills, and respiratory rehabilitation may help slow the disease progression and control symptoms [5]. Drugs such as phosphodiesterase type 4 inhibitors, corticosteroids, and 2-agonists are currently used for treatment. However, existing medicines cannot stop disease development or prevent drug intolerance and severe adverse effects. Side effects of bronchodilators or steroids used for therapy include dry mouth, headache, weight gain, and easy bruising. Long-term use of these drugs can lead to

intolerance, in which case they are no longer effective in slowing disease progression [6]. There is therefore a need to identify additional treatments for COPD that have high efficacy and low toxicity.

Jakyakgamcho-tang (JGT) is an Asian herbal formula that consists of *Paeoniae Radix* (*Paeonia lactiflora* Pallas) and *Glycyrrhizae Radix et Rhizoma* (*Glycyrrhiza uralensis* Fischer). As demonstrated, JGT has analgesic [7], antispasmodic [8], anti-allergy effects [9], and anti-inflammatory [10]. Analysis by gas chromatography/mass spectroscopy found ten main active ingredients of JGT: albiflorin, oxypaeoniflorin, ononin, isoliquiritin, glycyrrhizin, benzoic acid, liquiritin, gallic acid, benzoylpaeoniflorin, and paeoniflorin [11]. Glycyrol, a benzofuran coumarin from *G. uralensis*, was shown to have anti-inflammatory effects [12], and glycyrrhizin, a related compound, was found to prevent the replication of severe acute respiratory syndrome coronavirus (SARS-CoV) [13]. Moreover, evidence from an in vitro model showed that gancaonin N, a prenylated isoflavone from *G. uralensis*, ameliorated the inflammatory response associated with acute pneumonia [14], and studies in animal models found that the total glucosides of *P. lactiflora* regulated immune responses and had anti-inflammatory effects [15,16]. In addition, an extract of *P. lactiflora* was found to inhibit the human respiratory syncytial virus (HRSV) in vitro [17], and to have anti-influenza activity in vivo [18]. However, there have been no previous studies examining the efficacy of JGT for COPD. This research therefore tested the influences of JGT on COPD in mice induced by CS and lipopolysaccharide (LPS).

2. Materials and Methods

2.1. Quantitative Analysis of JGT by HPLC

Each of the nine reference standards for JGT received from ChemFaces Biochemical (Wuhan, China) has a purity of 98% or above. These standards were used in high-performance liquid chromatography (HPLC) for quantitative analysis of JGT. The JGT water extract was dissolved in methanol and adjusted to a 5 mg/mL before being filtered. To obtain standard mixtures for quantitative analysis, methanol was used to mix and dilute the stock solutions of the nine reference standards. The nine JGT compounds were quantitatively analyzed by using a Waters Alliance e2695 HPCL system (Waters Corporation, Milford, MA, USA) outfitted with an ultraviolet (UV) photodiode array (PDA) detector (Waters Corp.) with a wavelength range of 190–400 nm. Chromatographic separation was performed using a 0.1% (*v/v*) aqueous FA gradient solvent system and acetonitrile at 30 °C with a Sunfire C18 Column (Waters Corp.). The flow rate was 1 mL/min, and the gradient elution was 5 to 55% B for 0 to 35 min, 55 to 100% B for 35 to 40 min, 100% B for 40 to 46 min, and 5% B for 47 to 55 min. Each sample was injected at 10 µL and all data were analyzed with Empower software version 3 (Waters Corp.).

2.2. Induction of COPD Mice Model

Six-week-old male C57BL/6 mice (Orient Bio Inc., Seongnam-si, Korea) used in the experiments were kept in experimental animal breeding facility in Chungnam National University. Up until testing, the animals were acclimated and provided standard rodent food and sterilized tap water. The mice were separated into 5 groups (*n* = 8/group): (1) normal control (NC), (2) CS with intranasal LPS (COPD), (3) CS with intranasal LPS plus 5 mg/kg roflumilast by oral gavage as positive control (RO), (4) CS with intranasal LPS plus 100 mg/kg (human dose: 8.11 mg/kg) JGT by oral gavage (JGT-100), and (5) CS with intranasal LPS plus 200 mg/kg (human dose: 16.22 mg/kg) JGT by oral gavage (JGT-200). Mice in the NC group received saline instead of LPS, and mice in the four COPD groups were exposed in CS and LPS. The Tobacco and Health Research Institute at University of Kentucky provided 3R4F research cigarettes, which were used to produce CS. In the exposure chamber, mice inhaled CS of 8 cigarettes for 1 h daily for 8 weeks. LPS (10 µg) was administered by intranasal instillation under anesthesia at four different times (weeks 1, 3, 5, and 7). Beginning in week 4, mice in the three therapy groups were given 5 mg/kg roflumilast (RO), 100 mg/kg JGT (JGT-100), or 200 mg/kg JGT (JGT-200) 1 h before each CS

exposure (Figure 1). All mice were sacrificed at week 8. The Animal Experimental Ethics Committee at Chungnam National University authorized the animal research (Daejeon, Republic of Korea; Approval Number: CNU-01141).

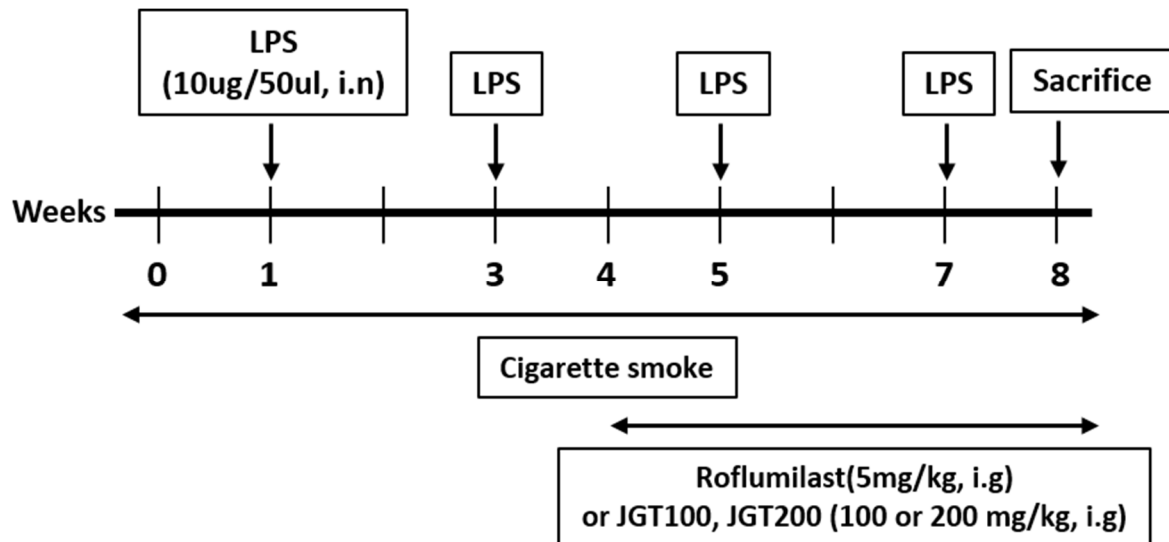


Figure 1. Experimental procedure for the introduction of COPD in mice and treatment with JGT.

2.3. Bronchoalveolar Lavage Fluid (BALF) Collection and Enzyme-Linked Immunosorbent Assay (ELISA)

Following the last CS challenge, mice were sacrificed 48 h later. BALF was collected from the whole lungs by instilling and withdrawing of DPBS through a tracheal cannula, performing three times. Trypan blue staining was used to exclude dead cells before counting cells. On a slide with BALF, the cells were fixed, dried, and stained by using Diff-Quik Stain reagents (IMEB Inc., San Marcos, CA, USA). TNF- α and IL-6 level in BALF were determined by ELISA kits (R&D System, Minneapolis, MN, USA). These data are presented as pg/mL protein.

2.4. Histopathological Examination

Lung tissue was fixed, paraffin embedded, and sectioned with a microtome. Deparaffinized sections are stained with hematoxylin and eosin (H&E), then dehydrated, mounted, and analyzed under a microscope. According to the above description, the level of inflammatory cell infiltration was graded from 0 (absent) to 4 (severe) [19]. The mean linear intercept (MLI) was calculated from 5 images of 4 animals in each group at random to investigate lung changes [20]. At 20 \times magnification, five equally spaced horizontal lines were examined. The sum of all estimated lines was then divided by the sum of intercepts per field. Collagen deposition in lung tissue was investigated by staining paraffin sections with Sirius red and counterstaining with Mayer's hematoxylin.

2.5. Real-Time Polymerase Chain Reaction (RT-PCR)

To isolate total RNA from lung samples, a homogenizer and the TRIZOL reagent (Invitrogen, CA, USA) were employed. The complementary DNA templates were synthesized and RT-PCR was performed by using the primer in Table 1. These results were normalized to GAPDH and relative quantitation was assessed by the $2^{-\Delta\Delta C_t}$ method.

Table 1. Primers used to amplify target genes.

| Gene | Primer |
|--------------------------------|---|
| <i>IL-1β</i> | F: 5'-AAAAAAGCCTCGTGCTGTCG-3' R: 5'-GTCGTTGCTTGGTTCCTCTG-3' |
| <i>IL-6</i> | F: 5'-TCCATCCAGTTGCCCTTCTTG-3' R: 5'-TTCCACGATTTCCCAGAGAAC-3' |
| <i>TNF-α</i> | F: 5'-AAGCCTGTAGCCACGTCGTA-3' R: 5'-AGGTACAACCCATCGGCTGG-3' |
| <i>MCP-1</i> | F: 5'-GCATCCACGTGTTGGCTCA-3' R: 5'-CTCCAGCCTACTCATTGGGATCA-3' |
| <i>TGF-β</i> | F: 5'-TTGCTTCAGCTCCACAGAGA-3' R: 5'-TGGTTGTAGAGGGCAAGGAC-3' |
| <i>α-SMA</i> | F: 5'-TAGGCACGTTGTGAGTCACACCA-3' R: 5'-CGACACTGCTGACAGAGGCACCA-3' |
| <i>MMP-9</i> | F: 5'-GTTTTTGATGCATTTGCTGAGATCCA-3' R: 5'-CCCACATTTGACGTCCAGAGAAGAA-3' |
| <i>GAPDH</i> | F: 5'-TCGTGGATCTGACGTGCCGCCTG-3' R: 5'-CACCACCCTGTTGCTGTAGCCGTAT-3' |

2.6. Western Blot Analysis

After homogenizing the lung tissues in a RIPA Buffer (Cell Signaling Technology, Danvers, MA, USA), centrifugation was used to remove debris. The BCA assay was used to quantify proteins. On 8% SDS-PAGE gels, equal quantities of total lung proteins (20 μ g) were separated and transferred to membranes. The membrane was incubated with primary antibodies after blocking. Following washing, a suitable secondary antibody was applied to the membrane. Protein expression was measured using the EzWestLumi plus system (ATTO Corporation, Tokyo, Japan), and levels were quantified relative to β -actin using CSAnalyzer 4.

2.7. Statistical Analysis

The data are described resented as means \pm standard errors of mean (SEM). A one-way analysis of variance (ANOVA) was used to conduct statistical comparisons in Prism 6 (Graphpad, San Diego, CA, USA). A *p* value of 0.05 or less was considered significant.

3. Results

3.1. Simultaneous Quantification of the Nine Compounds in JGT

The HPLC technique was improved for the simultaneous measurement of the nine compounds contained in JGT water extract (Figure 2A,B). The wavelengths used for quantitative analysis were 230 nm (albiflorin, benzoic acid, benzoylpaeoniflorin, and paeoniflorin); 250 nm (glycyrrhizin); and 275 nm (gallic acid, liquiritin apioside, liquiritigenin, and liquiritin). By using a mobile phase of 0.1% (*v/v*) aqueous FA and acetonitrile, we effectively separated these nine compounds in 35 min. The retention times were 6.44 min (gallic acid), 14.28 min (albiflorin), 15.12 min (paeoniflorin), 16.71 min (liquiritin apioside), 17.21 min (liquiritin), 21.51 min (benzoic acid), 24.58 min (liquiritigenin), 26.20 min (benzoylpaeoniflorin), and 34.62 min (glycyrrhizin). The calibration of each reference standard was calculated by the correlation between peak area (*y*) and concentration (*x*, μ g/mL) of the standard mixture, and determined from a linear regression equation ($y = ax + b$; Table 2). The linear ranges were 12.5 to 400 μ g/mL (paeoniflorin); 3.125 to 100 μ g/mL (gallic acid, liquiritin apioside, liquiritin, and glycyrrhizin); 1.5625 to 50 μ g/mL (albiflorin, benzoic acid, and benzoylpaeoniflorin); and 0.39 to 12.5 μ g/mL (liquiritigenin). The correlation coefficient for each compound indicated good linearity ($r^2 \geq 0.9999$). The limit of detection (LOD) and limit of quantification (LOQ) ranged from 0.014 to 0.587 μ g/mL and 0.041 to

1.780 µg/mL, respectively. The amount of each compound in the water extract of JGT ranged from 0.222 mg/g (liquiritigenin) to 55.292 mg/g (paeoniflorin).

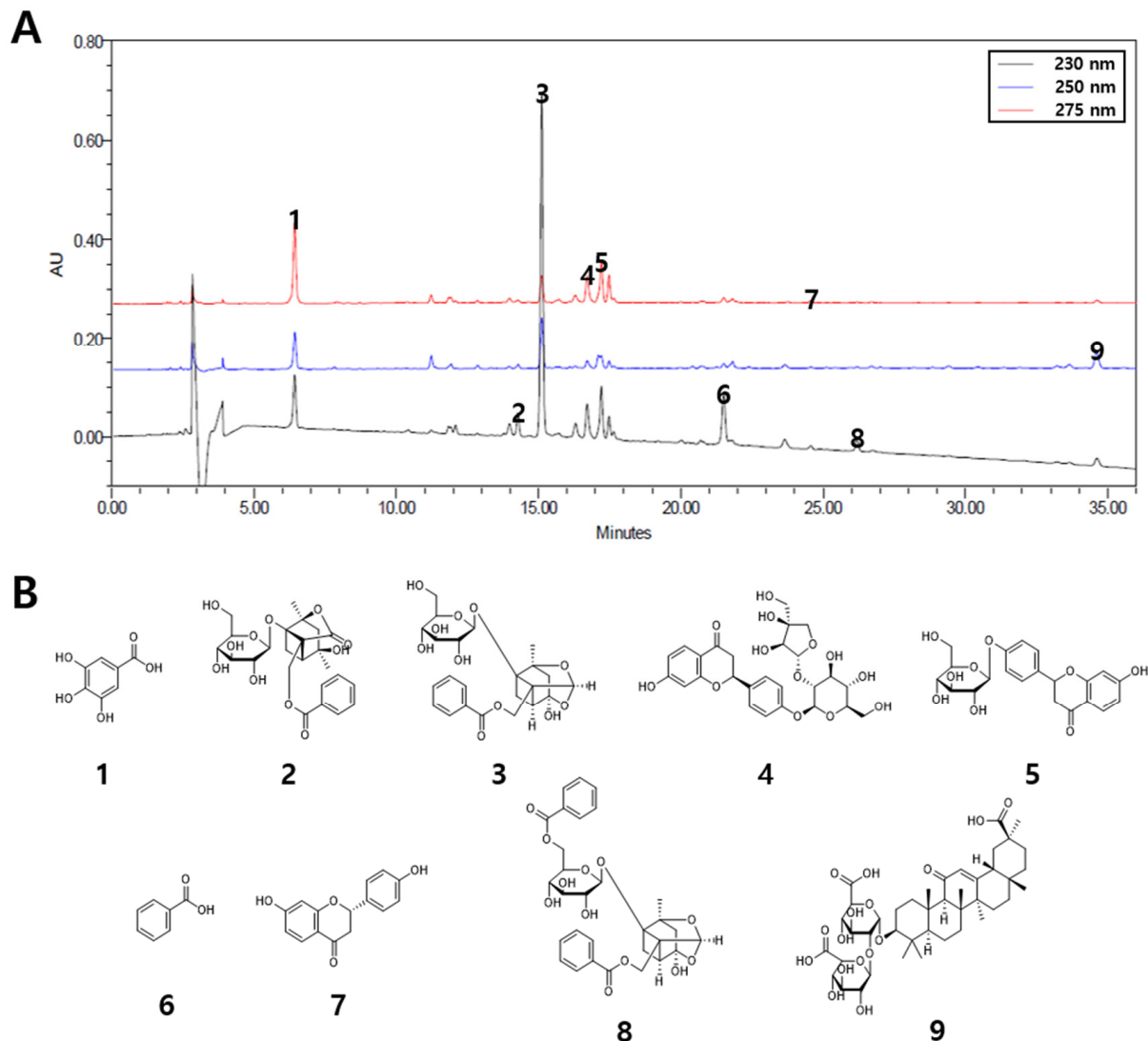


Figure 2. Simultaneous quantification of nine compounds in JGT. (A) HPLC chromatograms of the water extract of JGT at 230, 250, and 275 nm. (B) Chemical structures of the nine compounds. 1, gallic acid; 2, albiflorin; 3, paeoniflorin; 4, liquiritin apioside; 5, liquiritin; 6, benzoic acid; 7, liquiritigenin; 8, benzoylpaeoniflorin; 9, glycyrrhizin.

Table 2. Regression parameters, LOD, LOQ, and concentrations of the nine compounds in JGT.

| Compound | Linear Range (µg/mL) | Regression Equation ^a | | Correlation Coefficient (r ²) | LOD ^b (µg/mL) | LOQ ^c (µg/mL) | Concentration (mg/g) |
|---------------------|----------------------|----------------------------------|---------------|---|--------------------------|--------------------------|----------------------|
| | | Slope (a) | Intercept (b) | | | | |
| Gallic acid | 3.125~100 | 28,401 | −9804.2 | 0.9999 | 0.042 | 0.126 | 8.665 ± 0.008 |
| Albiflorin | 1.5625~50 | 13,499 | −895.32 | 1.0000 | 0.096 | 0.289 | 5.089 ± 0.030 |
| Paeoniflorin | 12.5~400 | 16,167 | 717.8 | 1.0000 | 0.587 | 1.780 | 55.292 ± 0.111 |
| Liquiritin apioside | 3.125~100 | 14,801 | 2361.4 | 1.0000 | 0.112 | 0.340 | 5.977 ± 0.031 |
| Liquiritin | 3.125~100 | 18,962 | 2978.4 | 1.0000 | 0.150 | 0.453 | 6.279 ± 0.010 |
| Benzoic acid | 1.5625~50 | 52,232 | 6550.1 | 1.0000 | 0.150 | 0.455 | 3.497 ± 0.002 |
| Liquiritigenin | 0.39~12.5 | 36,568 | 528.46 | 1.0000 | 0.014 | 0.041 | 0.222 ± 0.001 |
| Benzoylpaeoniflorin | 1.5625~50 | 25,762 | 762.53 | 1.0000 | 0.087 | 0.264 | 1.603 ± 0.009 |
| Glycyrrhizin | 3.125~100 | 6315.4 | 125.64 | 1.0000 | 0.103 | 0.311 | 10.492 ± 0.030 |

^a Regression equation was from $y = ax + b$, where y is the peak area, x is the mean concentration (µg/mL), a is the slope, and b is the intercept. ^b LOD: $3.3 \times$ (standard deviation [SD] of the response/slope of the calibration curve). ^c LOQ: $10 \times$ (SD of the response/slope of the calibration curve).

3.2. Effects of JGT on Histological Injury in Lung Tissues

Lung tissue of mice was stained with H&E in order to determine if JGT has any impact on histopathological alterations caused on COPD. In comparison to NC mice, COPD mice had severe immune cell infiltration in the peribronchiolar lesion (Figure 3A,B) and increased average alveolar intercepts (Figure 3C), indicating the degree of emphysema. By contrast, treatment with RO or JGT reduced inflammatory cell infiltration and average alveolar intercept.

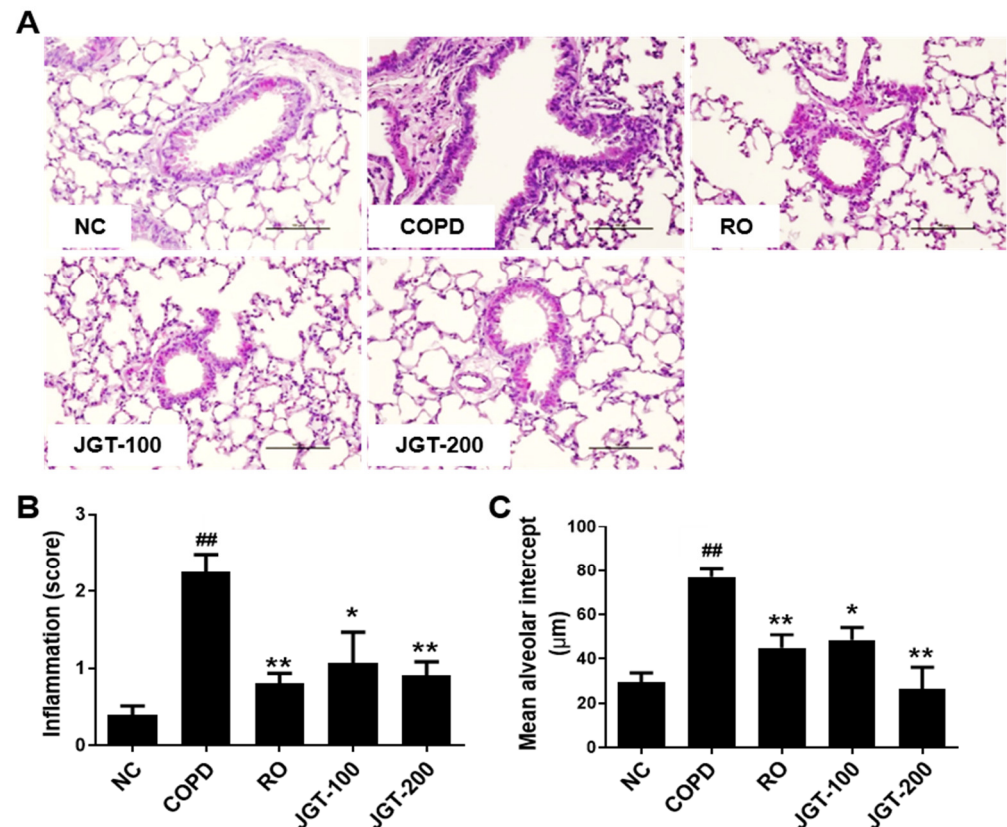


Figure 3. Effect of JGT on histological change. (A) H&E staining. (B) The degree of inflammation. (C) Average alveolar intercept. Lung tissue samples were fixed, sectioned, stained with H&E, and analyzed microscopically. NC, normal control mice; COPD, CS, & LPS-treated mice; RO, roflumilast (5 mg/kg) along with CS & LPS-treated mice; JGT-100, JGT (100 mg/kg) along with CS & LPS-treated mice; JGT-200, JGT (200 mg/kg) along with CS & LPS-treated mice. Data are displayed as means \pm SEM. ^{##} $p < 0.01$ compared with NC; ^{*} $p < 0.05$ and ^{**} $p < 0.01$ compared with COPD.

3.3. Effects of JGT on BALF Inflammatory Cells

We studied the efficacy of JGT on COPD-induced lung inflammation by using changes in total cells, lymphocytes, and macrophages in BALF. The COPD group had considerably more total cells (Figure 4A), lymphocytes (Figure 4B), and macrophages (Figure 4C) than the NC group. In COPD mice treated with 200 mg/kg JGT, the quantity of inflammatory cells was significantly reduced (Figure 4).

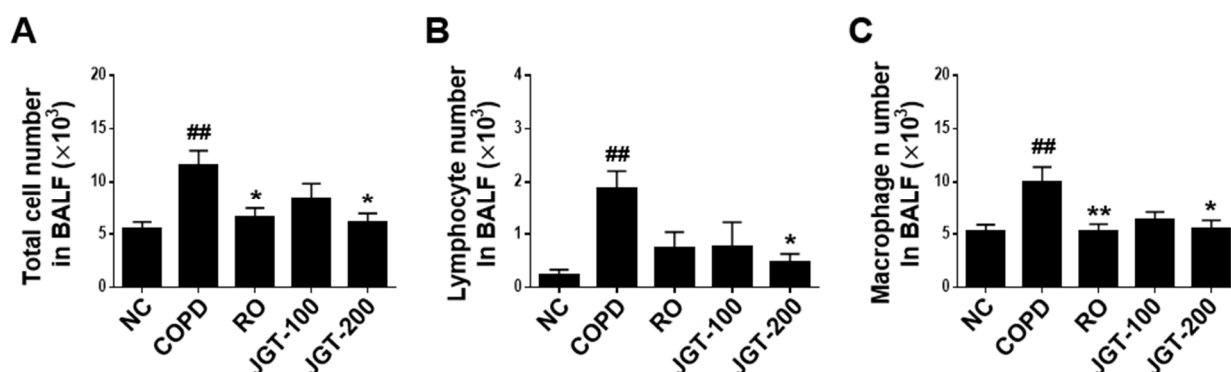


Figure 4. Effects of JGT on inflammatory cell counts in BALF. (A) Numbers of total inflammatory cells. (B) Numbers of lymphocytes. (C) Numbers of macrophages. NC, normal control mice; COPD, CS & LPS-treated mice; RO, roflumilast (5 mg/kg) along with CS & LPS-treated mice; JGT-100, JGT (100 mg/kg) along with CS & LPS-treated mice; JGT-200, JGT (200 mg/kg) along with CS & LPS-treated mice. Data are displayed as means \pm SEM. ^{##} $p < 0.01$ compared with NC; ^{*} $p < 0.05$ and ^{**} $p < 0.01$ compared with COPD.

3.4. Effects of JGT on TNF- α and IL-6 Levels in BALF

To see if JGT influences cytokine secretion into BALF, we assessed TNF- α and IL-6 concentrations by using ELISA. TNF- α and IL-6 levels in COPD mice were substantially greater than in NC animals (Figure 5). JGT treatment obviously reduced TNF- α (Figure 5A) and IL-6 (Figure 5B) levels in COPD mice BALF. Although not statistically significant, the RO treatment reduced cytokine secretions in the BALF of COPD mice (Figure 5).

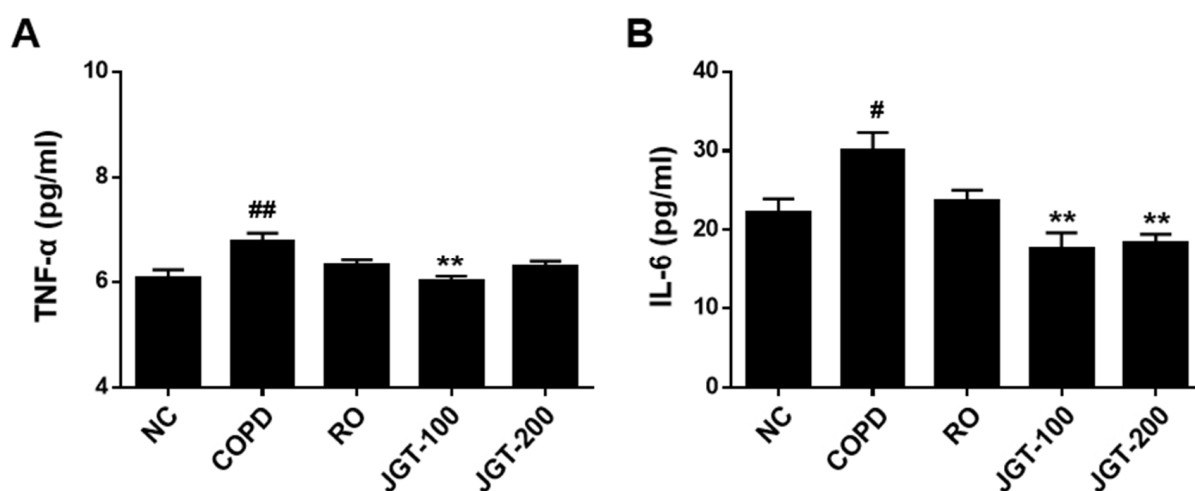


Figure 5. Effects of JGT on proinflammatory cytokine concentrations. (A) TNF- α and (B) IL-6 in BALF, as detected by ELISA. NC, normal control mice; COPD, CS & LPS-treated mice; RO, roflumilast (5 mg/kg) along with CS & LPS-treated mice; JGT-100, JGT (100 mg/kg) along with CS & LPS-treated mice; JGT-200, JGT (200 mg/kg) along with CS & LPS-treated mice. Data are displayed as means \pm SEM. [#] $p < 0.05$ and ^{##} $p < 0.01$ compared with NC; ^{**} $p < 0.01$ compared with COPD.

3.5. Effects of JGT on Proinflammatory Cytokines and Chemokines Levels in Lung Tissues

An increase in inflammatory cytokines particularly enhances the expression of many inflammatory genes in COPD. By using RT-PCR, the effects of JGT on the synthesis of these proinflammatory cytokines were assessed. COPD mice had significantly higher mRNA levels than the NC group (Figure 5). Increased TNF- α (Figure 6A), IL-6 (Figure 6B), IL-1 β (Figure 6C), and MCP-1 (Figure 6D) levels were diminished in JGT-treated mice.

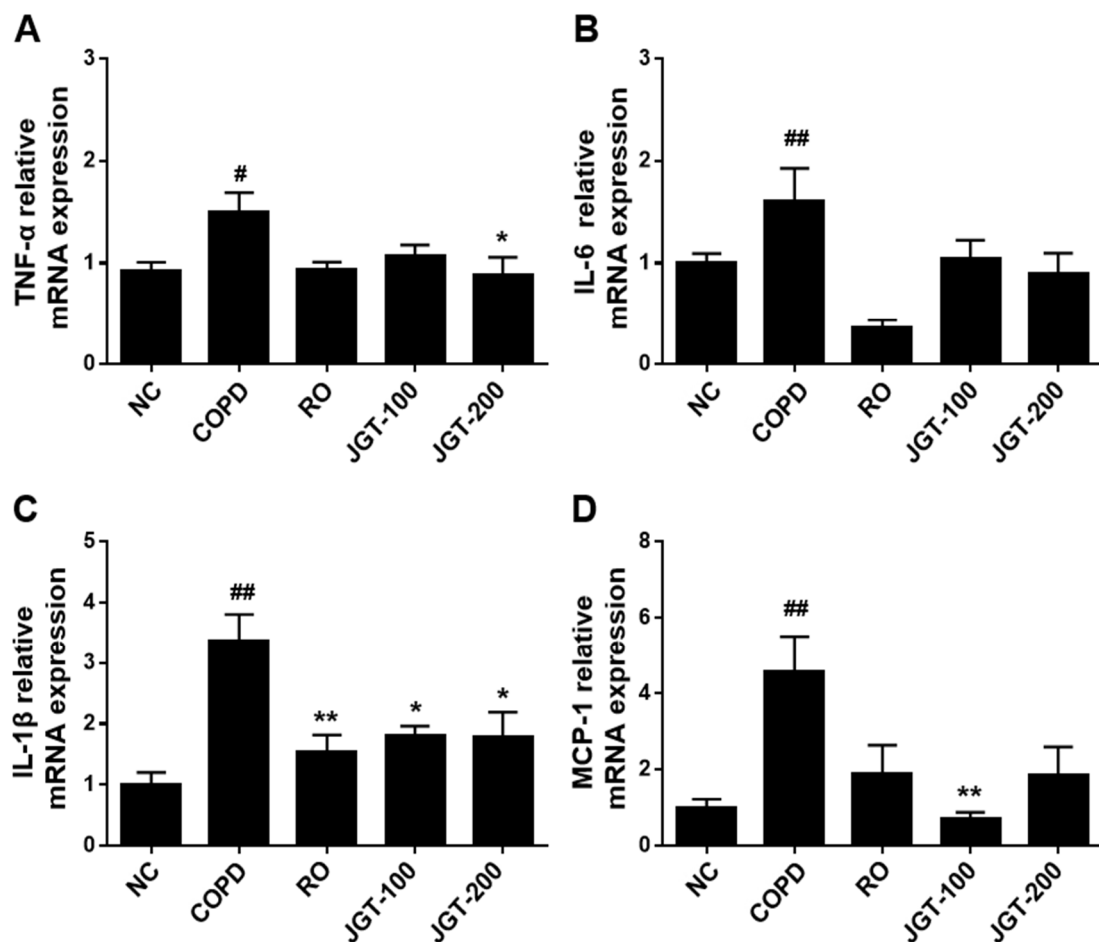


Figure 6. Effects of JGT on the concentrations of mRNAs encoding the proinflammatory cytokines (A) TNF- α , (B) IL-6, (C) IL-1 β , and (D) MCP-1 in lung tissue, as measured by real-time RT-PCR. NC, normal control mice; COPD, CS & LPS-treated mice; RO, roflumilast (5 mg/kg) along with CS & LPS-treated mice; JGT-100, JGT (100 mg/kg) along with CS & LPS-treated mice; JGT-200, JGT (200 mg/kg) along with CS & LPS-treated mice. Data are displayed as means \pm SEM. # $p < 0.05$ and ## $p < 0.01$ compared with NC; * $p < 0.05$ and ** $p < 0.01$ compared with COPD.

3.6. Effects of JGT on Lung Tissue Remodeling

Airway walls and alveoli constricted by tissue remodeling are significant pathologic features of COPD [21]. Increased peri-bronchiolar fibrosis and interstitial extracellular matrix (ECM) deposition are two of the most significant structural changes in COPD lung tissue. To examine the effects of JGT on structural changes of the lung, we performed histological examination and assessed the relative mRNA expression levels of relevant genes. Increased peribronchiolar collagen deposition was found in the COPD tissue by Sirius-red staining, which was significantly reduced in RO or JGT treated-mice (Figure 7A). Moreover, the mRNA levels of TGF- β (Figure 7B), α -SMA (Figure 7C), and MMP-9 (Figure 7D) were increased in the COPD than in the NC (Figure 7), but these increases were markedly reduced by RO or JGT treatment (Figure 7).

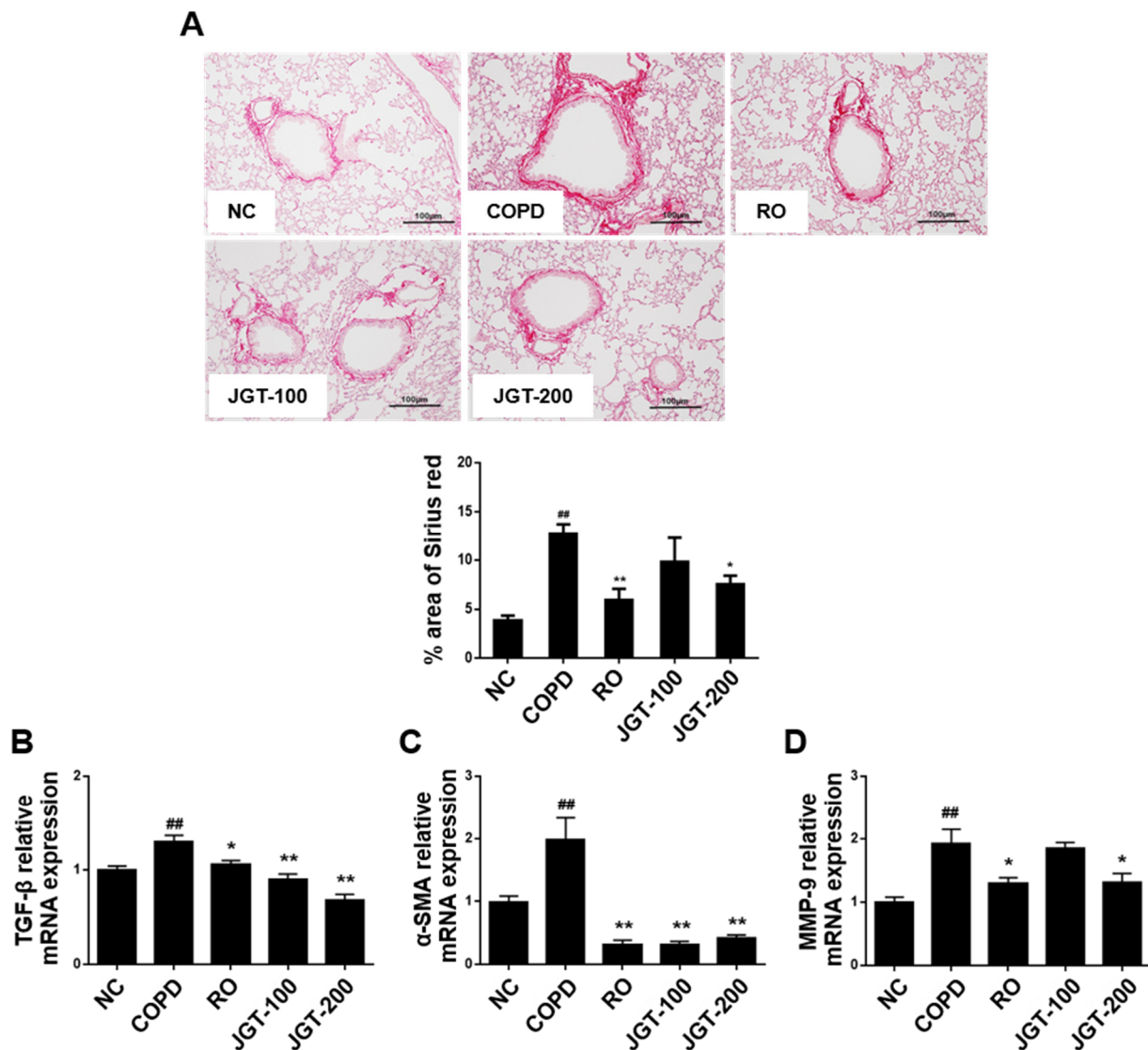


Figure 7. Effects of JGT on (A) the collagen deposition and the levels of (B) TGF- β , (C) α -SMA, and (D) MMP-9 mRNAs, as measured by RT-PCR. NC, normal control mice; COPD, CS & LPS-treated mice; RO, roflumilast (5 mg/kg) along with CS & LPS-treated mice; JGT-100, JGT (100 mg/kg) along with CS & LPS-treated mice; JGT-200, JGT (200 mg/kg) along with CS & LPS-treated mice. Data are displayed as means \pm SEM. ^{##} $p < 0.01$ compared with NC; ^{*} $p < 0.05$ and ^{**} $p < 0.01$ compared with COPD.

3.7. Effects of JGT on the Phosphorylation of NF- κ B, ERK1/2, and p38 MAPKs in Lung Tissues

The effects of JGT on COPD-induced signaling pathways were investigated by measuring NF- κ B and MAPK phosphorylation levels. Phosphorylated NF- κ B, ERK1/2, and p38 MAPKs were increased in the COPD more so than in the NC (Figure 8). When COPD mice were provided RO or JGT treatments, these increases were noticeably reduced.

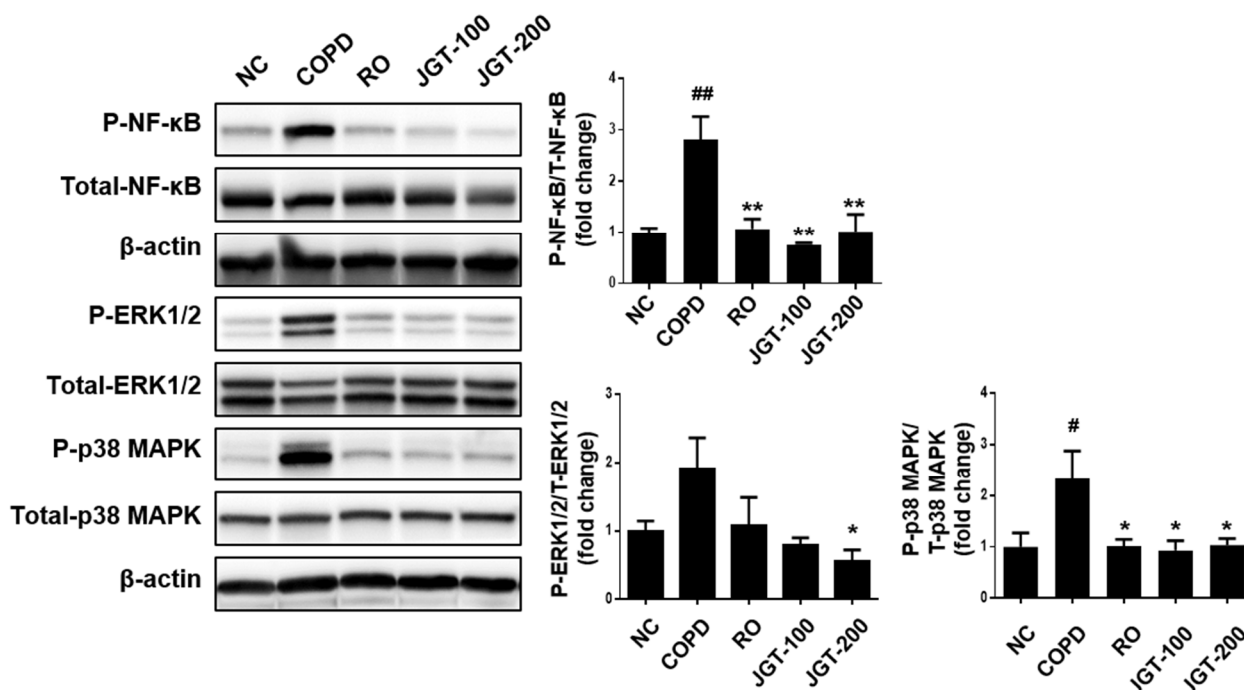


Figure 8. Effects of JGT on activations of NF- κ B, ERK1/2, and p-38 in lung tissues, according to Western blot analysis. NC, normal control mice; COPD, CS & LPS-treated mice; RO, roflumilast (5 mg/kg) along with CS & LPS-treated mice; JGT-100, JGT (100 mg/kg) along with CS & LPS-treated mice; JGT-200, JGT (200 mg/kg) along with CS & LPS-treated mice. Data are displayed as means \pm SEM. # $p < 0.05$ and ## $p < 0.01$ compared with NC; * $p < 0.05$ and ** $p < 0.01$ compared with COPD.

4. Discussion

Herbal medicines are gaining popularity due to their potential therapeutic efficacy and fewer side effects. For thousands of years, well-known herbal medications have been commonly given for a variety of diseases. The present research used a CS and LPS-induced COPD mouse disease model to explore the efficacy of JGT on the pathogenesis of COPD. JGT treatment considerably decreased production of proinflammatory cytokines and infiltration of inflammatory cells in lung tissue and BALF of CS and LPS-induced COPD mouse models. Treatment with JGT also markedly hindered COPD-induced increases in TGF- β , α -SMA, and MMP-9. In addition, phosphorylation of NF- κ B, ERK1/2, and p38 MAPKs is found to decrease following treatment of JGT.

Paeonia lactiflora Pallas and *Glycyrrhiza uralensis* Fischer comprise JGT. The major elements of JGT are monoterpene glycosides, monoterpenes, and carboxylic acids from *Paeoniae Radix* and triterpenes, flavanones, and flavonoid glycosides from *Glycyrrhizae Radix et Rhizoma* [22]. In our data, quantitative determination of the concentrations of nine compounds in water extracts of JGT—albiflorin, gallic acid, liquiritin apioside, liquiritin, benzoic acid, liquiritigenin, benzoylpaeoniflorin, glycyrrhizin, and paeoniflorin—by HPLC-PDA showed that paeoniflorin (55.292 mg/g) was the most abundant compound. Anti-inflammatory properties of JGT components have been demonstrated. *Glycyrrhiza uralensis* Fischer's roots and rhizomes have been used to cure dermatitis, peptic ulcer, and bronchitis [23]. Furthermore, it was discovered that it can reduce asthma symptoms by lowering airway hypersensitivity responses and oxidative stress [24]. *Paeonia lactiflora* Pallas has also been shown to be effective in treating inflammatory airway disorders such as COPD and asthma [25].

Clinically, COPD is associated with chronic airway inflammation caused by inflammatory cell activity inside lung tissue. When exposed to pollutants that are breathed, such as cigarette smoke (CS), a key contributing factor to COPD, these cells become activated. CS

causes airway remodeling and permanent pathological alterations in the lungs including emphysema [26]. Because chronic inflammation persists even after stopping smoking, an unregulated and persistent inflammatory response can lead to lung tissue destruction and remodeling [27]. This chronic inflammation caused by infiltration into the lungs of inflammatory cells, which produce proinflammatory cytokines and chemokines. This study found that JGT treatment substantially reduced the increased number of inflammatory cells as well as cytokine and chemokine levels due to CS and LPS in BALF and lung tissues.

The expression of several proinflammatory genes is increased as a result of the up-regulation of TNF- α , IL-1, and IL-6 in COPD, which has been demonstrated to enhance inflammation by activating NF- κ B [28]. The immune system and inflammatory responses are regulated by the NF- κ B pathway, a transcriptional regulator [29]. The cytoplasm contains an inactive NF- κ B molecule bound to I κ B. NF- κ B is dissociated from I κ B and transferred to the nucleus after stimulation, where it induces the production of inflammatory cytokines and inducible enzymes [30]. A variety of cells express inflammatory cytokines and other inflammatory mediators under the control of the MAPKs signaling pathway [31]. Phosphorylation of molecules in NF- κ B and MAPKs pathways can be readily observed in inflammatory lung disorders such as pneumonia and COPD [32]. The pathogenesis of COPD with immune infiltration, mucus overproduction, fibrosis, and airway remodeling and inflammation is associated with JNK, ERK1/2, and p38 MAPKs [33]. ERK1/2 is implicated in pathological disease such as chronic inflammation and cancer and is concerned with cell growth, survival, migration, proliferation, and differentiation [34]. p38 MAPK is intimately linked to inflammation and is required for the generation of IL-1 β , IL-6, and TNF- α [35]. This study showed that JGT reduced NF- κ B, ERK1/2, and p38 MAPK phosphorylation levels in COPD-induced lung tissues, suggesting that JGT reduces inflammation by preventing NF- κ B and MAPKs signaling pathway activation.

Histological examination of biopsy specimens from COPD patients has revealed structural abnormalities, such as airway wall thickening, subepithelial fibrosis, and increases in smooth muscle mass [36]. Fibroblast growth factor (FGF), TNF- α , insulin-like growth factor (IGF), IL-8, and peculiarly, TGF- β are essential elements in this process [37]. TGF- β has been shown to increase collagen and fibronectin production by fibroblasts, suggesting its importance in the progression of peribronchial fibrosis. According to research, TGF- β has been related to smooth muscle cell proliferation and mucus hypersecretion [38–40]. MMP-9, a member of the MMP family, is generated by smooth myocytes, mast cells, epithelial cells, and fibroblasts, all of which are significant mediators of the extracellular matrix metabolism and airway wall remodeling [41,42]. Expression of MMP-9 is also higher in several types of lung cells of individuals with IPF (idiopathic pulmonary fibrosis) [43]. MMP-9 is the most potent profibrotic mediator and has a bidirectional connection with TGF- β 1. As a reaction to TGF- β 1 generated in the lung epithelium, IPF lung fibroblasts produce MMP-9, which in turn activates latent TGF- β 1 to increase the active TGF- β 1 pool [44]. Peribronchial fibrosis following airway remodeling is thus most likely the result of a TGF- β -mediated process comparable to uncontrolled repair. The current investigation discovered that JGT therapy significantly lowered increased levels of TGF- β and MMP-9 in LPS and CS—exposed mice, indicating that the beneficial impact of JGT on COPD may potentially be connected to airway remodeling. Notably, prior studies have shown that NF- κ B and MAPKs signaling regulate MMP-9 expression. MMP-9 expression is promoted by the IL-1 β and TNF- α through NF- κ B, ERK1/2, and p38 MAPK signaling pathway [42,45]. JGT inhibits airway remodeling caused by CS and LPS-induced COPD via partially regulating the phosphorylation of NF- κ B, ERK1/2, and p38 MAPKs.

5. Conclusions

JGT therapy effectively decreased CS and LPS-induced COPD in mice by diminishing inflammatory cytokines and airway remodeling. These effects of JGT were associated with decreased activation of NF- κ B, p38 MAPK, and ERK1/2. These findings suggest that JGT may be a viable COPD treatment option. Even though JGT showed the similar effects with

Roflumilast, the first drug for the treatment of COPD, further study is needed to evaluate the clinical value of JGT.

Author Contributions: Methodology, Y.-J.K. and E.-J.H.; conceptualization, H.-J.K. and M.-Y.L.; formal analysis, J.H.K., E.B.B., and E.-J.H.; investigation, J.H.K. and E.B.B.; resources, Y.-J.K.; writing—review and editing, H.-J.K. and J.H.K.; funding acquisition, H.-J.K. and M.-Y.L.; writing—original draft preparation, H.-J.K. and J.H.K.; project administration, H.-J.K. and M.-Y.L.; supervision, H.-J.K. All authors have read and agreed to the published version of the manuscript.

Funding: The Korea Institute of Oriental Medicine funded this study with grants number KSN2013220 and KSN2021220.

Institutional Review Board Statement: Chungnam National University's Animal Experimental Ethics Committee approved the animal study protocol (CNU-01141 and 19 December 2018).

Data Availability Statement: On request, the corresponding author can provide access to the data described in this study.

Conflicts of Interest: The authors declare no conflict of interest.

References

1. Vestbo, J.; Hurd, S.S.; Agustí, A.G.; Jones, P.W.; Vogelmeier, C.; Anzueto, A.; Barnes, P.J.; Fabbri, L.M.; Martinez, F.J.; Nishimura, M. Global strategy for the diagnosis, management, and prevention of chronic obstructive pulmonary disease: GOLD executive summary. *Am. J. Respir. Crit. Care Med.* **2013**, *187*, 347–365. [[CrossRef](#)] [[PubMed](#)]
2. MacNee, W. Pathogenesis of chronic obstructive pulmonary disease. *Proc. Am. Thorac. Soc.* **2005**, *2*, 258–266. [[CrossRef](#)] [[PubMed](#)]
3. Chouchane, S.; Wooten, J.B.; Tewes, F.J.; Wittig, A.; Müller, B.P.; Veltel, D.; Diekmann, J. Involvement of semiquinone radicals in the in vitro cytotoxicity of cigarette mainstream smoke. *Chem. Res. Toxicol.* **2006**, *19*, 1602–1610. [[CrossRef](#)] [[PubMed](#)]
4. De Cunto, G.; Cavarra, E.; Bartalesi, B.; Lucattelli, M.; Lungarella, G. Innate Immunity and Cell Surface Receptors in the Pathogenesis of COPD: Insights from Mouse Smoking Models. *Int. J. Chron. Obstruct. Pulmon. Dis.* **2020**, *15*, 1143–1154. [[CrossRef](#)] [[PubMed](#)]
5. Kew, K.M.; Dias, S.; Cates, C.J. Long-acting inhaled therapy (beta-agonists, anticholinergics and steroids) for COPD: A network meta-analysis. *Cochrane Database Syst. Rev.* **2014**, *3*. [[CrossRef](#)] [[PubMed](#)]
6. Alagha, K.; Palot, A.; Sofalvi, T.; Pahus, L.; Gouitaa, M.; Tummino, C.; Martinez, S.; Charpin, D.; Bourdin, A.; Chanez, P. Long-acting muscarinic receptor antagonists for the treatment of chronic airway diseases. *Ther. Adv. Chronic. Dis.* **2014**, *5*, 85–98. [[CrossRef](#)]
7. Sui, F.; Zhou, H.-Y.; Meng, J.; Du, X.-L.; Sui, Y.-P.; Zhou, Z.-K.; Dong, C.; Wang, Z.-J.; Wang, W.-H.; Dai, L. A Chinese herbal decoction, Shaoyao-Gancao Tang, exerts analgesic effect by down-regulating the TRPV1 channel in a rat model of arthritic pain. *Am. J. Chin. Med.* **2016**, *44*, 1363–1378. [[CrossRef](#)]
8. Kaifuchi, N.; Omiya, Y.; Kushida, H.; Fukutake, M.; Nishimura, H.; Kase, Y. Effects of shakuyakukanzoto and its absorbed components on twitch contractions induced by physiological Ca²⁺ release in rat skeletal muscle. *J. Nat. Med.* **2015**, *69*, 287–295. [[CrossRef](#)]
9. Shen, L.; Hu, R.-w.; Lin, X.; Cong, W.-j.; Hong, Y.-l.; Feng, Y.; Xu, D.-s.; Ruan, K.-f. Pharmacokinetics of characteristic effective ingredients from individual and combination Shaoyao and Gancao treatment in rats using HPLC fingerprinting. *Eur. J. Drug Metab. Pharmacokinet.* **2012**, *37*, 133–140. [[CrossRef](#)]
10. Shao, Y.-y.; Chang, Z.-p.; Cheng, Y.; Wang, X.-c.; Zhang, J.-p.; Feng, X.-j.; Guo, Y.-t.; Liu, J.-j.; Hou, R.-g. Shaoyao-Gancao decoction alleviated hyperandrogenism in a letrozole-induced rat model of polycystic ovary syndrome by inhibition of NF- κ B activation. *Biosci. Rep.* **2019**, *39*, BSR20181877. [[CrossRef](#)]
11. Seo, S.H.; Unno, T.; Park, S.E.; Kim, E.J.; Lee, Y.M.; Na, C.S.; Son, H.S. Korean Traditional Medicine (Jakyakgamcho-tang) Ameliorates Colitis by Regulating Gut Microbiota. *Metabolites* **2019**, *9*, 226. [[CrossRef](#)] [[PubMed](#)]
12. Shin, E.M.; Zhou, H.Y.; Guo, L.Y.; Kim, J.A.; Lee, S.H.; Merfort, I.; Kang, S.S.; Kim, H.S.; Kim, S.; Kim, Y.S. Anti-inflammatory effects of glycyrol isolated from *Glycyrrhiza uralensis* in LPS-stimulated RAW264.7 macrophages. *Int. Immunopharmacol.* **2008**, *8*, 1524–1532. [[CrossRef](#)]
13. Cinatl, J.; Morgenstern, B.; Bauer, G.; Chandra, P.; Rabenau, H.; Doerr, H. Glycyrrhizin, an active component of liquorice roots, and replication of SARS-associated coronavirus. *Lancet* **2003**, *361*, 2045–2046. [[CrossRef](#)]
14. Ko, H.M.; Lee, S.-H.; Jee, W.; Jung, J.H.; Kim, K.-I.; Jung, H.-J.; Jang, H.-J. Gancaonin N from *Glycyrrhiza uralensis* Attenuates the Inflammatory Response by Downregulating the NF- κ B/MAPK Pathway on an Acute Pneumonia In Vitro Model. *Pharmaceutics* **2021**, *13*, 1028. [[CrossRef](#)] [[PubMed](#)]
15. Li, P.-P.; Liu, D.-D.; Liu, Y.-J.; Song, S.-S.; Wang, Q.-T.; Chang, Y.; Wu, Y.-J.; Chen, J.-Y.; Zhao, W.-D.; Zhang, L.-L. BAFF/BAFF-R involved in antibodies production of rats with collagen-induced arthritis via PI3K-Akt-mTOR signaling and the regulation of paeoniflorin. *J. Ethnopharmacol.* **2012**, *141*, 290–300. [[CrossRef](#)] [[PubMed](#)]

16. Zhou, Z.; Lin, J.; Huo, R.; Huang, W.; Zhang, J.; Wang, L.; Sun, Y.; Shen, B.; Li, N. Total glucosides of paeony attenuated functional maturation of dendritic cells via blocking TLR4/5 signaling in vivo. *Int. Immunopharmacol.* **2012**, *14*, 275–282. [[CrossRef](#)] [[PubMed](#)]
17. Lin, T.-J.; Wang, K.-C.; Lin, C.-C.; Chiang, L.-C.; Chang, J.-S. Anti-viral activity of water extract of *Paeonia lactiflora pallas* against human respiratory syncytial virus in human respiratory tract cell lines. *Am. J. Chin. Med.* **2013**, *41*, 585–599. [[CrossRef](#)]
18. Ho, J.-Y.; Chang, H.-W.; Lin, C.-F.; Liu, C.-J.; Hsieh, C.-F.; Horng, J.-T. Characterization of the anti-influenza activity of the Chinese herbal plant *Paeonia lactiflora*. *Viruses* **2014**, *6*, 1861–1875. [[CrossRef](#)]
19. Gori, S.; Alcain, J.; Vanzulli, S.; Moreno Ayala, M.A.; Candolfi, M.; Jancic, C.; Geffner, J.; Vermeulen, M.; Salamone, G. Acetylcholine-treated murine dendritic cells promote inflammatory lung injury. *PLoS ONE* **2019**, *14*, e0212911. [[CrossRef](#)]
20. Rho, J.; Seo, C.-S.; Hong, E.-J.; Baek, E.B.; Jung, E.; Park, S.; Lee, M.-Y.; Kwun, H.-J. Yijjin-Tang Attenuates Cigarette Smoke and Lipopolysaccharide-Induced Chronic Obstructive Pulmonary Disease in Mice. *Evid. Based. Complement. Alternat. Med.* **2022**, *2022*, 7902920. [[CrossRef](#)]
21. Grzela, K.; Litwiniuk, M.; Zagorska, W.; Grzela, T. Airway remodeling in chronic obstructive pulmonary disease and asthma: The role of matrix metalloproteinase-9. *Arch. Immunol. Ther. Exp.* **2016**, *64*, 47–55. [[CrossRef](#)] [[PubMed](#)]
22. Zhou, J.-X.; Braun, M.S.; Wetterauer, P.; Wetterauer, B.; Wink, M. Antioxidant, cytotoxic, and antimicrobial activities of *Glycyrrhiza glabra* L., *Paeonia lactiflora* Pall., and *Eriobotrya japonica* (Thunb.) Lindl. extracts. *Medicines* **2019**, *6*, 43. [[CrossRef](#)] [[PubMed](#)]
23. Wang, L.; Zhang, K.; Han, S.; Zhang, L.; Bai, H.; Bao, F.; Zeng, Y.; Wang, J.; Du, H.; Liu, Y. Constituents isolated from the leaves of *Glycyrrhiza uralensis* and their anti-inflammatory activities on LPS-induced RAW264. 7 cells. *Molecules* **2019**, *24*, 1923. [[CrossRef](#)] [[PubMed](#)]
24. Huang, W.-C.; Liu, C.-Y.; Shen, S.-C.; Chen, L.-C.; Yeh, K.-W.; Liu, S.-H.; Liou, C.-J. Protective effects of licochalcone A improve airway hyper-responsiveness and oxidative stress in a mouse model of asthma. *Cells* **2019**, *8*, 617. [[CrossRef](#)] [[PubMed](#)]
25. Ryu, H.W.; Song, H.-H.; Shin, I.-S.; Cho, B.O.; Jeong, S.H.; Kim, D.-Y.; Ahn, K.-S.; Oh, S.-R. Suffruticosol A isolated from *Paeonia lactiflora* seedcases attenuates airway inflammation in mice induced by cigarette smoke and LPS exposure. *J. Funct. Foods* **2015**, *17*, 774–784. [[CrossRef](#)]
26. Tuder, R.M.; Yun, J.H. It takes two to tango: Cigarette smoke partners with viruses to promote emphysema. *J. Clin. Investig.* **2008**, *118*, 2689–2693. [[CrossRef](#)]
27. Cowburn, A.S.; Condliffe, A.M.; Farahi, N.; Summers, C.; Chilvers, E.R. Advances in neutrophil biology: Clinical implications. *Chest.* **2008**, *134*, 606–612. [[CrossRef](#)]
28. Barnes, P.J. The cytokine network in chronic obstructive pulmonary disease. *Am. J. Respir. Cell Mol. Biol.* **2009**, *41*, 631–638. [[CrossRef](#)]
29. Li, Q.; Verma, I.M. NF- κ B regulation in the immune system. *Nat. Rev. Immunol.* **2002**, *2*, 725–734. [[CrossRef](#)]
30. Liang, Y.; Zhou, Y.; Shen, P. NF- κ B and its regulation on the immune system. *Cell Mol. Immunol.* **2004**, *1*, 343–350.
31. Kaminska, B. MAPK signalling pathways as molecular targets for anti-inflammatory therapy—from molecular mechanisms to therapeutic benefits. *Biochim. Biophys. Acta. Proteins Proteom.* **2005**, *1754*, 253–262. [[CrossRef](#)] [[PubMed](#)]
32. Wong, J.; Magun, B.E.; Wood, L.J. Lung inflammation caused by inhaled toxicants: A review. *Int. J. Chron. Obstruct. Pulmon. Dis.* **2016**, *11*, 1391. [[CrossRef](#)] [[PubMed](#)]
33. Mercer, B.A.; D’Armiento, J.M. Emerging role of MAP kinase pathways as therapeutic targets in COPD. *Int. J. Chron. Obstruct. Pulmon. Dis.* **2006**, *1*, 137. [[CrossRef](#)] [[PubMed](#)]
34. Sun, Y.; Liu, W.-Z.; Liu, T.; Feng, X.; Yang, N.; Zhou, H.-F. Signaling pathway of MAPK/ERK in cell proliferation, differentiation, migration, senescence and apoptosis. *J. Recept. Signal Transduct.* **2015**, *35*, 600–604. [[CrossRef](#)] [[PubMed](#)]
35. Suzuki, M.; Tetsuka, T.; Yoshida, S.; Watanabe, N.; Kobayashi, M.; Matsui, N.; Okamoto, T. The role of p38 mitogen-activated protein kinase in IL-6 and IL-8 production from the TNF- α - or IL-1 β -stimulated rheumatoid synovial fibroblasts. *FEBS Lett.* **2000**, *465*, 23–27. [[CrossRef](#)]
36. Jeffery, P.K. Remodeling and inflammation of bronchi in asthma and chronic obstructive pulmonary disease. *Proc. Am. Thorac. Soc.* **2004**, *1*, 176–183. [[CrossRef](#)]
37. Holgate, S.; Lackie, P.; Davies, D.; Roche, W.; Walls, A. The bronchial epithelium as a key regulator of airway inflammation and remodelling in asthma. *Clin. Exp. Immunol.* **1999**, *29*, 90–95. [[CrossRef](#)]
38. McMillan, S.J.; Xanthou, G.; Lloyd, C.M. Manipulation of allergen-induced airway remodeling by treatment with anti-TGF- β antibody: Effect on the Smad signaling pathway. *J. Immunol.* **2005**, *174*, 5774–5780. [[CrossRef](#)]
39. Panettieri Jr, R.A.; Kotlikoff, M.I.; Gerthoffer, W.T.; Hershenson, M.B.; Woodruff, P.G.; Hall, I.P.; Banks-Schlegel, S. Airway smooth muscle in bronchial tone, inflammation, and remodeling: Basic knowledge to clinical relevance. *Am. J. Respir. Crit. Care Med.* **2008**, *177*, 248–252. [[CrossRef](#)]
40. Xie, S.; Sukkar, M.B.; Issa, R.; Khorasani, N.M.; Chung, K.F. Mechanisms of induction of airway smooth muscle hyperplasia by transforming growth factor- β . *Am. J. Physiol. Lung Cell Mol. Physiol.* **2007**, *293*, L245–L253. [[CrossRef](#)]
41. Abel, M.; Vliagoftis, H. Mast cell-fibroblast interactions induce matrix metalloproteinase-9 release from fibroblasts: Role for IgE-mediated mast cell activation. *J. Immunol.* **2008**, *180*, 3543–3550. [[CrossRef](#)] [[PubMed](#)]
42. Liang, K.C.; Lee, C.W.; Lin, W.N.; Lin, C.C.; Wu, C.B.; Luo, S.F.; Yang, C.M. Interleukin-1 β induces MMP-9 expression via p42/p44 MAPK, p38 MAPK, JNK, and nuclear factor- κ B signaling pathways in human tracheal smooth muscle cells. *J. Cell. Physiol.* **2007**, *211*, 759–770. [[CrossRef](#)] [[PubMed](#)]

43. Pardo, A.; Cabrera, S.; Maldonado, M.; Selman, M. Role of matrix metalloproteinases in the pathogenesis of idiopathic pulmonary fibrosis. *Respir. Res.* **2016**, *17*, 23. [[CrossRef](#)]
44. Ramírez, G.; Hagood, J.S.; Sanders, Y.; Ramírez, R.; Becerril, C.; Segura, L.; Barrera, L.; Selman, M.; Pardo, A. Absence of Thy-1 results in TGF- β induced MMP-9 expression and confers a profibrotic phenotype to human lung fibroblasts. *Lab. Investig.* **2011**, *91*, 1206–1218. [[CrossRef](#)] [[PubMed](#)]
45. Lin, C.-C.; Tseng, H.-W.; Hsieh, H.-L.; Lee, C.-W.; Wu, C.-Y.; Cheng, C.-Y.; Yang, C.-M. Tumor necrosis factor- α induces MMP-9 expression via p42/p44 MAPK, JNK, and nuclear factor- κ B in A549 cells. *Toxicol. Appl. Pharmacol.* **2008**, *229*, 386–398. [[CrossRef](#)]